Detection of Proteins and Protein−Ligand Complexes Using HgTe Nanostructure Matrixes in Surface-Assisted Laser Desorption/Ionization Mass Spectrometry

ARTICLE *in* ANALYTICAL CHEMISTRY · JUNE 2010

Impact Factor: 5.64 · DOI: 10.1021/ac100550c · Source: PubMed

6 AUTHORS, INCLUDING:

Cheng-Kang Chiang
University of Ottawa
25 PUBLICATIONS **907** CITATIONS
SEE PROFILE

Yang-Wei Lin
National Changhua University of Education
62 PUBLICATIONS **1,561** CITATIONS
SEE PROFILE

Han-Jia Lin
National Taiwan Ocean University
27 PUBLICATIONS **274** CITATIONS
SEE PROFILE

Huan-Tsung Chang
National Taiwan University
297 PUBLICATIONS **10,214** CITATIONS
SEE PROFILE

Anal. Chem. **2010,** *82,* 4543–4550

Detection of Proteins and Protein−Ligand Complexes Using HgTe Nanostructure Matrixes in Surface-Assisted Laser Desorption/Ionization Mass Spectrometry

Cheng-Kang Chiang,[†] Zusing Yang,[†] Yang-Wei Lin,[†] Wen-Tsen Chen,[†] Han-Jia Lin,[‡] and Huan-Tsung Chang*,[†]

Department of Chemistry, National Taiwan University, 1, Section 4, Roosevelt Road, Taipei 106, Taiwan, and Institute of Bioscience and Biotechnology, National Taiwan Ocean University, 2 Pei-Ning Road, Keelung, Taiwan

We have analyzed peptides, proteins, and protein−drug complexes through surface-assisted laser desorption/ionization mass spectrometry (SALDI-MS) using HgTe nanostructures as matrixes. We investigated the effects of several parameters, including the concentration of the HgTe nanostructures, the pH of the buffer, and the concentration of salt, on the performance of this system. When HgTe nanostructures are used as matrixes, $[M + H]^+$ ions were the dominant signals. Relative to other commonly used nanomaterials, HgTe nanostructures provided lower background signals from metal clusters, fewer fragment ions, less interference from alkali-adducted analyte ions, and a higher mass range (up to 150 000 Da). The present approach provides limits of detection for angiotensin I and bovine serum albumin of 200 pM and 14 nM, respectively, with great reproducibility (RSD: <25%). We validated the applicability of this method through the detections of (i) the recombinant proteins that were transformed in *E. coli*, (ii) the specific complex between bovine serum albumin and L-tryptophan, and (iii) a carbonic anhydrase−acetazolamide complex. Our results suggest that this novel and simple SALDI-MS approach using HgTe nanostructures as matrixes might open several new ways for proteomics and the analysis of drug−protein complexes.

Matrix-assisted laser desorption/ionization mass spectrometry (MALDI-MS) is a commonly used, powerful tool for the rapid quantification and identification of large biomolecules, including proteins, peptides, and nucleic acids.[1] Rapid energy transfer from UV-absorbing matrixes allows analytes to undergo soft and efficient desorption and ionization with minimal degrees of fragmentation. Unfortunately, inhomogeneous crystallization of analytes within organic matrixes commonly creates "sweet spots" during MALDI-MS analyses, with associated problems of low accuracy and poor shot-to-shot and sample-to-sample reproducibility.[2]

Detection of noncovalent complexes is difficult when MALDI-MS is used, primarily because the classic matrixes [e.g., sinapinic acid (SA)], typical additives (e.g., trifluoroacetic acid), and commonly used organic solvents (e.g., acetonitrile) tend to disrupt weakly bound complexes under laser irradiation.[3] Therefore, unlike electrospray ionization (ESI), MALDI is rarely used for the mass spectrometric detection of weak protein complexes. Only a few MALDI-MS approaches using less acidic matrixes, such as 6-aza-2-thiothymine (ATT),[4] 2,4,6-trihydroxyacetophenone (THAP),[5] and 3-hydroxypicolinic acid (HPA),[4b,5c] have been demonstrated for the detection of protein−protein,[4a,5a,b] protein−DNA,[4b] and protein−peptide[5c] complexes. Nevertheless, special experimental conditions must be selected to minimize the dissociation of the intact complexes and the formation of nonspecific aggregates when these less acidic matrixes are employed for MALDI-MS.

Surface-assisted laser desorption/ionization mass spectrometry (SALDI-MS) using nanomaterials as matrixes has recently been developed for the determination of various analytes of interest.[6] Several inorganic materials have been employed as SALDI-MS matrixes, including graphite,[6,7] porous silicon and alumina,[8]

* To whom correspondence should be addressed. Tel/Fax: 011-886-2-33661171. E-mail: changht@ntu.edu.tw.

[†] National Taiwan University.

[‡] National Taiwan Ocean University.

(1) (a) Karas, M.; Hillenkamp, F. *Anal. Chem.* **1988**, *60*, 2299–2301. (b) Tanaka, K.; Waki, H.; Ido, Y.; Akita, S.; Yoshida, Y.; Yoshida, T. *Rapid Commun. Mass Spectrom.* **1988**, *2*, 151–153.

(2) (a) Scherzer, W.; Selzle, H. L.; Schlag, E. W. *Chem. Phys. Lett.* **1992**, *195*, 11–15. (b) Tholey, A.; Heinzle, E. *Anal. Bioanal. Chem.* **2006**, *386*, 24–37.

(3) (a) Farmer, T. B.; Caprioli, R. M. *J. Mass Spectrom.* **1998**, *33*, 697–704. (b) Jecklin, M. C.; Schauer, S.; Dumelin, C. E.; Zenobi, R. *J. Mol. Recognit.* **2009**, *22*, 319–329.

(4) (a) Glocker, M. O.; Bauer, S. H. J.; Kast, J.; Volz, J.; Przybylski, M. *J. Mass Spectrom.* **1996**, *31*, 1221–1227. (b) Tang, X.; Callahan, J. H.; Zhou, P.; Vertes, A. *Anal. Chem.* **1995**, *67*, 4542–4548.

(5) (a) Cohen, L. R. H.; Strupat, K.; Hillenkamp, F. *J. Am. Soc. Mass Spectrom.* **1997**, *8*, 1046–1052. (b) Rosinke, B.; Strupat, K.; Hillenkamp, F.; Rosenbusch, J.; Dencher, N.; Krüger, U.; Galla, H.-J. *J. Mass Spectrom.* **1995**, *30*, 1462–1468. (c) Jespersen, S.; Niessen, W. M. A.; Tjaden, U. R.; van der Greef, J. *J. Mass Spectrom.* **1998**, *33*, 1088–1093.

(6) Sunner, J.; Dratz, E.; Chen, Y.-C. *Anal. Chem.* **1995**, *67*, 4335–4342.

(7) (a) Amini, N.; Shariatgorji, M.; Thorsén, G. *J. Am. Soc. Mass Spectrom.* **2009**, *20*, 1207–1213. (b) Dale, M. J.; Knochenmuss, R.; Zenobi, R. *Anal. Chem.* **1996**, *68*, 3321–3329. (c) Ugarov, M. V.; Egan, T.; Khabashesku, D. V.; Schultz, J. A.; Peng, H. Q.; Khabashesku, V. N.; Furutani, H.; Prather, K. S.; Wang, H.-W. J.; Jackson, S. N.; Woods, A. S. *Anal. Chem.* **2004**, *76*, 6734–6742.

10.1021/ac100550c
Published on Web 05/03/2010

carbon nanotubes,[9] TiO_2 films,[10] and nanoparticles (NPs) of SiO_2,[11] ZnS,[12] TiO_2,[13] Fe_3O_4/TiO_2,[14] Pt,[15] Ge,[16] ZnO,[17] Au,[18] Ag,[19] and Fe_3O_4.[20] Similar to the role played by organic matrixes, these nanomaterials absorbed the energy of the laser pulse, leading to desorption of the analytes. Because of their unique chemical and physical properties, nanomaterials can also act as selective probes. For example, Au and TiO_2 NPs are suitable matrixes for the concentration and ionization of aminothiols and catechins, respectively, in SALDI-MS.[13,18b] Although these approaches provide better reproducibility and fewer sweet spots relative to MALDI-MS, the mass limit remains quite low (ca. 20 kDa).[15a]

In this study, we employed HgTe nanostructures as a new matrix for SALDI-MS-based analyses of proteins and their complexes with small analytes. We carefully evaluated what the roles of several parameters, including the concentration of HgTe nanostructures, the pH, and the concentration of salt, had on the sensitivity of the SALDI-MS technique toward proteins. We validated the practicality of SALDI-MS using the HgTe nanostructures for the detections of proteins having molecular weights of up to 150 000 Da, protein−drug complexes, and the recombinant proteins transformed in *E. coli*.

EXPERIMENTAL SECTION

Chemicals and Proteins. Mercury chloride ($HgCl_2$), tellurium powder, acetonitrile (ACN), ethanol (EtOH), THAP, HPA, and ammonium hydroxide (NH_4OH) were obtained from Acros (Geel, Belgium). Sodium borohydride ($NaBH_4$), mercaptopropionic acid (MPA), acetazolamide (ACZ), and citric acid were purchased from Aldrich (Milwaukee, WI). Angiotensin I, bovine serum albumin (BSA), cytochrome C, human carbonic anhydrase I (hCAI, EC 4.2.1.1), immunoglobulin G from human serum (IgG), insulin, L- and D-tryptophan (Y), SA, α-cyano-4-hydroxycinnamic acid (CHCA), trifluoroacetic acid (TFA), and all other chemicals were purchased from Sigma (St. Louis, MO). Citric acid (500 mM) and NH_4OH (25−30%) were used to prepare ammonium citrate solutions (100−500 mM, pH 4.0−9.0).

Synthesis of HgTe Nanostructures. Briefly, sodium hydrogen telluride (NaHTe) solution was prepared by mixing tellurium powder (0.127 g) and $NaBH_4$ solution (2 M, 1 mL) and incubating the mixture for 1 h prior to use. $HgCl_2$ (0.272 g), MPA solution (38 mM, pH 11.2, 74.8 mL), and the NaHTe solution (0.58 mL) were then mixed in a round-bottom flask and heated at 100 °C for 50 min. The instant color change, from grayish-brown to black, indicated the formation of HgTe nanostructures. The as-prepared HgTe nanostructures (1 mL) were then mixed with EtOH (0.5 mL). After stirring for 1 min, the mixtures were subjected to centrifugation (6000 rpm, 10 min) and the pellets were resuspended in deionized water (1 mL). For simplicity, the concentration of the purified HgTe nanostructures in each of the aqueous solutions is presented herein as 1×.

Characterization of HgTe Nanostructures. A Cintra 10e double-beam UV−vis spectrophotometer (GBC, Victoria, Australia) was used to measure the absorbance of the HgTe nanostructures (0.02×) in citrate solutions (300 mM, pH 5.0). High-resolution transmission electron microscopy (HR-TEM) images and energy-dispersive X-ray (EDX) spectra were recorded using an H7100 TEM system (Hitachi, Tokyo, Japan). The Zeta potential of the as-prepared HgTe nanostructures was recorded using a particles size analyzer (Zetasizer Nano, Malvern, UK). Prior to performing inductively coupled plasma mass spectrometry (ICPMS) measurements for the determination of the concentrations of Hg and Te, the HgTe nanostructures (50 μL) were first dissolved in aqua regia (950 μL) and then diluted with 2% HNO_3.

HgTe Nanostructures as Desorption/Ionization Matrixes. To optimize the experimental conditions for SALDI-MS using HgTe nanostructures as matrixes, BSA was used as a standard analyte. Aliquots of BSA solution (50 μM, 5 μL) were added separately to solutions containing HgTe nanostructures (5−30×, 10 μL), deionized water (5 μL), and 500 mM ammonium citrate solution (30 μL, pH 5.0), and then, the mixtures were equilibrated at ambient temperature for 30 min. Aliquots (1.0 μL) of the mixtures were separately pipetted onto a stainless-steel 96-well MALDI target (Bruker Daltonics) and dried in air at room temperature for 30 min prior to SALDI-MS analysis. The same SALDI-MS procedures were also applied using HgTe nanostructures (4×) to determine the linear range and limits of detection [LODs, at a signal-to-noise (S/N) ratio of 3] for various peptides and proteins, including angiotensin I, insulin, cytochrome C, hCA, BSA, and IgG. The concentration range for the analytes was 0.01−100 μM.

HgTe Nanostructures as Concentration Probes and Desorption/Ionization Matrixes. To further improve sensitivity, HgTe nanostructures were used as concentration and desorption/ionization matrixes. Sample solutions (1 mL) containing a peptide or protein, HgTe nanostructures (0.08×), and 300 mM ammonium citrate (pH 5.0) were equilibrated at ambient temperature for 30 min. The mixtures were then centrifuged (6000 rpm, 10 min), and

(8) (a) Finkel, N. H.; Prevo, B. G.; Velev, O. D.; He, L. *Anal. Chem.* **2005**, *77*, 1088–1095. (b) Tarui, A.; Kawasaki, H.; Taiko, T.; Watanabe, T.; Yonezawa, T.; Arakawa, R. *J. Nanosci. Nanotech.* **2009**, *9*, 159–164. (c) Wei, J.; Buriak, J. M.; Siuzdak, G. *Nature* **1999**, *399*, 243–246. (d) Wada, Y.; Yanagishita, T.; Masuda, H. *Anal. Chem.* **2007**, *79*, 9122–9127.

(9) Xu, S.; Lin, Y.; Zou, H.; Qiu, J.; Gou, Z.; Guo, B. *Anal. Chem.* **2003**, *75*, 6191–6195.

(10) (a) Chen, C.-T.; Chen, Y.-C. *Rapid Commun. Mass Spectrom.* **2004**, *18*, 1956–1964. (b) Lo, C.-Y.; Lin, J.-Y.; Chen, W.-Y.; Chen, C.-T.; Chen, Y.-C. *J. Am. Soc. Mass Spectrom.* **2008**, *19*, 1014–1020.

(11) Dagan, S.; Hua, Y.; Boday, D. J.; Somogyi, A.; Wysocki, R. J.; Wysocki, V. H. *Int. J. Mass Spectrom.* **2009**, *283*, 200–205.

(12) Kailasa, S. K.; Kiran, K.; Wu, H.-F. *Anal. Chem.* **2008**, *80*, 9681–9688.

(13) Lee, K.-H.; Chiang, C.-K.; Lin, Z.-H.; Chang, H.-T. *Rapid Commun. Mass Spectrom.* **2007**, *21*, 2023–2030.

(14) Chen, C.-T.; Chen, Y.-C. *Anal. Chem.* **2005**, *77*, 5912–5919.

(15) (a) Kawasaki, H.; Yonezawa, T.; Watanabe, T.; Arakawa, R. *J. Phys. Chem. C* **2007**, *111*, 16278–16283. (b) Yonezawa, T.; Kawasaki, H.; Tarui, A.; Watanabe, T.; Arakawa, R.; Shimada, T.; Mafuné, F. *Anal. Sci.* **2009**, *25*, 339–346.

(16) Sato, H.; Nemoto, A.; Yamamoto, A.; Tao, H. *Rapid Commun. Mass Spectrom.* **2009**, *23*, 603–610.

(17) Watanabe, T.; Kawasaki, H.; Yonezawa, T.; Arakawa, R. *J. Mass Spectrom.* **2008**, *43*, 1063–1071.

(18) (a) Castellana, E. T.; Russell, D. H. *Nano Lett.* **2007**, *7*, 3023–3025. (b) Huang, Y.-F.; Chang, H.-T. *Anal. Chem.* **2006**, *78*, 1485–1493. (c) Huang, Y.-F.; Chang, H.-T. *Anal. Chem.* **2007**, *79*, 4852–4859. (d) McLean, J. A.; Stumpo, K. A.; Russell, D. H. *J. Am. Chem. Soc.* **2005**, *127*, 5304–5305. (e) Chiang, C.-K.; Chiang, N.-C.; Lin, Z.-H.; Lan, G.-Y.; Chang, H.-T. *J. Am. Soc. Mass Spectrom.* **2010**, in press.

(19) (a) Chiu, T.-C.; Chang, L.-C.; Chiang, C.-K.; Chang, H.-T. *J. Am. Soc. Mass Spectrom.* **2008**, *19*, 1343–1346. (b) Shrivas, K.; Wu, H.-F. *Rapid Commun. Mass Spectrom.* **2008**, *22*, 2863–2872.

(20) Chen, W.-Y.; Chen, Y.-C. *Anal. Bioanal. Chem.* **2006**, *386*, 699–704.

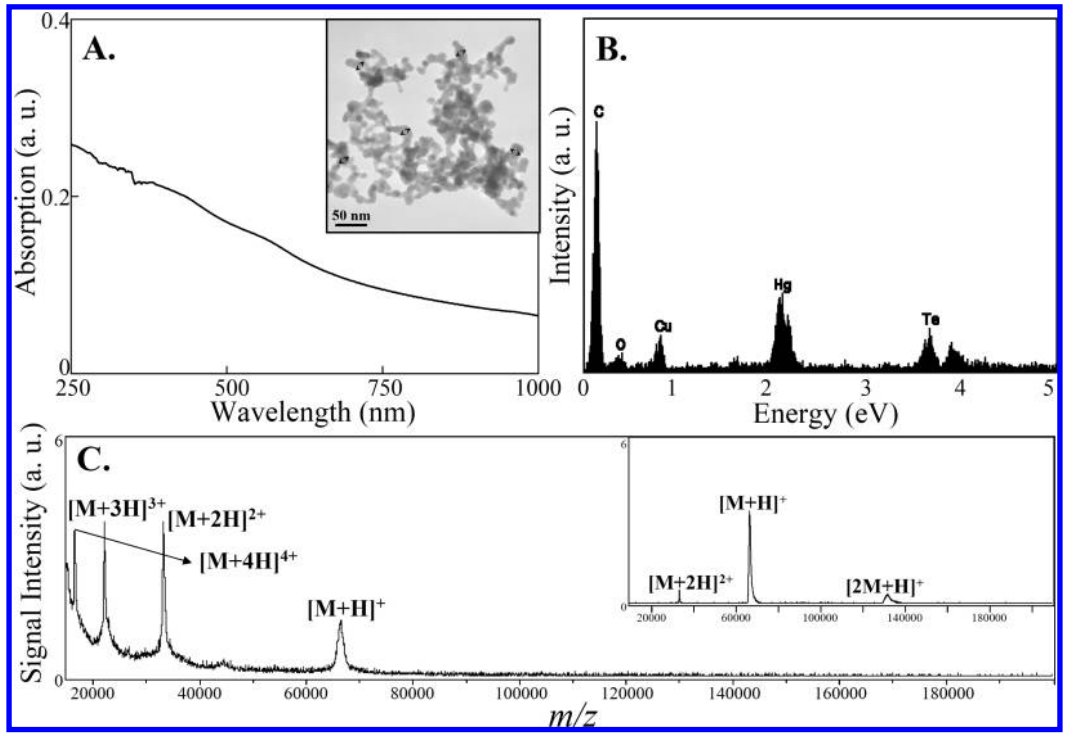

Figure 1. (A) UV−vis spectra of the as-prepared HgTe nanostructures. Inset: TEM image of the HgTe nanostructures. (B) EDX spectrum of the HgTe nanostructures. (C) Mass spectrum of BSA (5 μM) recorded using a matrix of HgTe nanostructures (4×) prepared in 300 mM ammonium citrate (pH 5.0). The signals at *m/z* 66 431, 33 216, 22 144, and 16 609 represent the adducts $[M + H]^+$, $[M + 2H]^{2+}$, $[M + 3H]^{3+}$, and $[M + 4H]^{4+}$, respectively. Inset: Mass spectrum of BSA obtained in SA matrixes (20 mg/mL in water/ACN (1:1, v/v) containing 0.1% TFA). The signals at *m/z* 132 862, 66 431, and 33 216 represent the adducts $[2\ M + H]^+$, $[M + H]^+$, and $[M + 2H]^{2+}$, respectively. SALDI-MS was performed in the linear mode. A total of 300 pulsed laser shots were applied under a laser pulse energy set at 62.5 μJ (power density on the sample substrate was estimated to be 2×10^9 W/cm^2).

all the supernatants were removed. The pellets were resuspended in ammonium citrate buffer (20 μL), and the sample solutions (1 μL) were pipetted onto a stainless steel target plate and allowed to air-dry for 30 min prior to SALDI-MS measurement.

Preparation of Recombinant Proteins zSSAT1 and zSSAT1 R101A. The coding sequence of zSSAT1(zgc:114142, GSPEFMANFNLRKAEPKDVPDILRLIKELAKYEEMEDQVLIT EKDLLEDGFGEHPFYHCVVADVSAEHQKVEGYS VIGFAMYY-FTYDPWIGKLLYLEDFYVMKEYRGFGIGSE ILKHLSDTAVKNR CSSMHFIVAESNKTSIDFYKRRGASDLSLQEGWRLFRIDKEN LLK-MSAEELEHHHHHH) was amplified from the cDNA prepared from the total RNA of a 72 h zebra fish embryo. The amplified cDNA was ligated into pGEX-2T vector (GE Healthcare Bioscience, NJ) via *Eco*RI and XhoI sites. The recombinant plasmid was also used as a template to produce zSSAT1 R101A cDNA, which encodes alanine instead of arginine at residue 101 of the cDNA, using a Quickchange mutagenesis kit (Stratagene, CA). Both the recombinant plasmids were transformed individually into *E. coli* strain BL21. To produce recombinant proteins, each *E. coli* clone was cultured at 37 °C overnight and subcultured with 10 times the volume of fresh Luria−Bertani (LB) medium until the value of OD600 reached 0.6. Isopropyl β-D-1-thiogalactopyranoside (0.5 mM) was then added to the culture, which continued growing at 37 °C for 5 h to induce the expression of recombinant proteins. The cell pallets were collected through centrifugation (1000*g*, 20 min) and lysed through ultrasonication (Microson XL2000, Misonix, NY) to obtain the crude protein extracts. The recombinant proteins were then purified through GSTrap HP affinity chromatography (GE Healthcare Bioscience, NJ) according to the manufacturer's instructions. The purified proteins were subjected to SALDI-MS analysis using HgTe nanostructures as matrixes. The sample preparation for SALDI-MS analysis was the same as that described for the standard protein samples.

Investigation of Protein−Drug Complexes. Prior to detection of BSA-Y complex ions by SALDI-MS, 300 mM ammonium citrate solutions (pH 5.0, 10 μL) containing BSA (10 μM), L-Y, or D-Y (0−200 μM) were equilibrated for 30 min. Aliquots of the solutions (10 μL) were then mixed separately with solutions containing HgTe nanostructures (8×) prepared in 300 mM ammonium citrate (pH 5.0). The mixtures were equilibrated for another 10 min. Sample solutions containing hCAI−ACZ complexes were prepared by mixing hCAI (100 μM, 1 μL), ACZ (0−2 mM, 1 μL), deionized water (4 μL), and 500 mM ammonium citrate (4 μL, pH 7.4). The mixtures were equilibrated for 30 min prior to addition of HgTe nanostructures (8×, 10 μL) in the presence of 0.01% Triton X-100. The mixtures were equilibrated for 10 min prior to SALDI-MS analysis.

SALDI-MS. Mass spectrometry experiments were performed in the linear or reflectron positive-ion mode using a Microflex MALDI-TOF mass spectrometer (Bruker Daltonics, Bremen, Germany). The samples were irradiated with a nitrogen laser (output at 337 nm) at 10 Hz. Ions produced by laser desorption were stabilized energetically during a delayed extraction period of 900 ns and then accelerated through the time-of-flight chamber

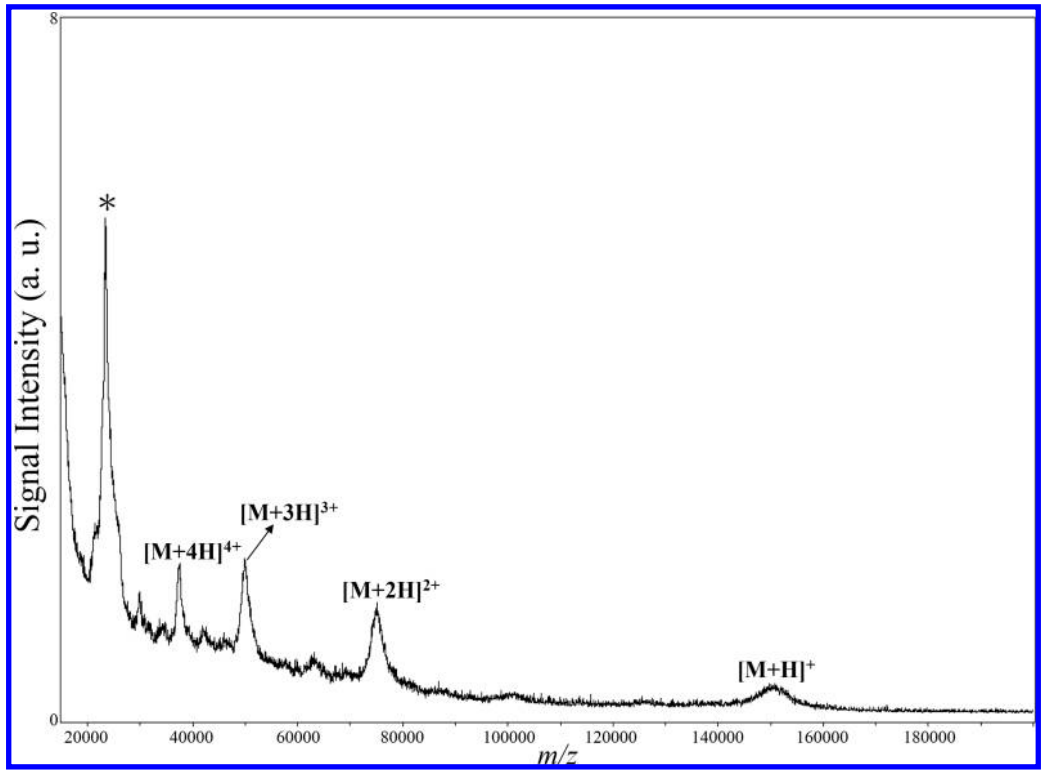

Figure 2. Mass spectrum of a solution containing IgG (5 μM) and HgTe nanostructures prepared in 300 mM ammonium citrate (pH 5.0). SALDI-MS was performed in the linear mode. The peaks at m/z 149 993, 75 012, 49 990, and 37 502 represent the adducts $[M + H]^+$, $[M + 2H]^{2+}$, $[M + 3H]^{3+}$, and $[M + 4H]^{4+}$, respectively. Other conditions were the same as those described in Figure 1.

in the reflectron or linear mode prior to entering the mass analyzer. The available accelerating voltages were in the range from +20 to −20 kV. To obtain good resolution and high S/N ratios, the laser energy was adjusted to slightly higher than the threshold and each mass spectrum was generated by averaging over 300 laser pulses. SALDI-MS experiments were performed in reflectron and linear modes for the analytes having m/z of <5000 and >5000, respectively.

RESULTS AND DISCUSSION

Characterization of HgTe Nanostructures. We synthesized HgTe nanostructures from Hg and Te salts at an Hg/Te molar ratio of 1:1. Figure 1A reveals that the HgTe products absorbed light over 200−1000 nm, suggesting that they would absorb light effectively from the N_2 laser used in our SALDI-MS system. To further characterize the products, we recorded TEM images and EDX spectra. One representative TEM image (inset to Figure 1A) reveals that the HgTe nanostructures had a network structure formed from the connection of many nanoscale structures (ca. 20 nm in diameter). The EDX pattern (Figure 1B) reveals the existence of Hg and Te elements. Using EDX spectroscopic and ICP mass spectrometric data (not shown), we confirmed that the product comprised HgTe nanostructures.

Parameters for MS Signals. We then tested the analysis of BSA through SALDI-MS using HgTe nanostructures. Figure 1C reveals that HgTe nanostructures provided apparent BSA signals and low background signals. The multiply charged ions at m/z 66 431, 33 216, 22 144, and 16 609 represent the $[M + H]^+$, $[M + 2H]^{2+}$, $[M + 3H]^{3+}$, and $[M + 4H]^{4+}$ adducts. On the other hand, MALDI-MS using SA matrixes prepared under acidic conditions allowed detections of $[M + H]^+$, $[M + 2H]^{2+}$, and $[2\ M + H]^+$ (m/z 132862). In addition, the SALDI-MS signal having the highest value of m/z was that of the $[M + H]^+$ ion, not $[M + Na]^+$, which appears commonly when other types of nanomaterials (e.g., Au NPs) are used. Thus, relative to other nanomaterials, the use of HgTe as the matrix provides less interference from alkali-adducted analyte ions (e.g., $[M + Na]^+$, $[M + K]^+$, and multiple salt adducts).[18a]

In addition, we found that BSA signals were absent when we used 14 nm Au NPs as the matrix.[18e] Because energy transfer between the nanostructures and analytes is likely to occur via a thermally driven process, it is preferable to employ matrixes having lower thermal conductivities to generate higher laser-induced temperatures.[15b] The thermal conductivities of elemental Au, Hg, and Te are 317, 8.34, and 2.35 W m^{-1} K^{-1}, respectively; in addition, the melting temperatures of elemental Hg and Te are much lower (234 and 723 K, respectively) than that (1337 K) of Au. Figure S-1 (Supporting Information) and Table S-1 (Supporting Information) reveal that several quasimolecular ions, including $[Te_x]^+$, $[Te_x + Hg + SH]^+$, and $[Te_x + S]^+$ adducts, were observed over the m/z range of 250−1200 Da when the HgTe nanomaterials were subjected to laser irradiation, in which $x = 2-9$. The ease of generation of these quasimolecular ions suggests that another advantage of the use of the HgTe nanomaterials as matrixes is that they might protect or maintain the protein structure during the ionization/desorption process.[8d] Taken together, our results reveal that HgTe

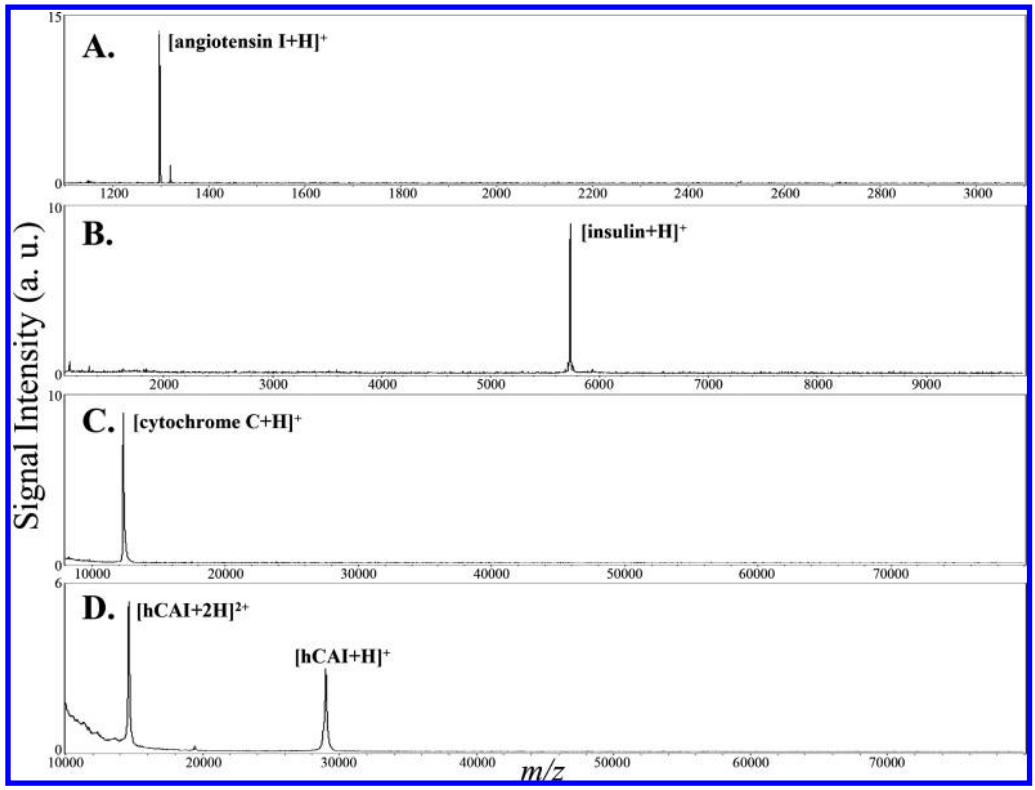

Figure 3. SALDI mass spectra recorded using HgTe nanostructures as the matrixes: (A) 100 nM angiotensin I; (B) 500 nM insulin; (C) 1 μM cytochrome C; (D) 1 μM hCAI. SALDI-MS experiments were performed in the reflectron mode for angiotensin I, while in the linear mode for the other analytes. The signals at *m/z* 1296.7, 5734.5, 12 361, 14 387, and 28 778 represent the adducts [angiotensin I + H]$^+$, [insulin + H]$^+$, [cytochrome C + H]$^+$, [hCAI + 2H]$^{2+}$, and [hCAI + H]$^+$, respectively. Other conditions were the same as those described in Figure 1.

nanostructures provide more efficient and softer desorption and ionization processes and fewer background ions.

Several factors, including the nanostructure and salt concentrations and the pH, influence the sensitivity of the SALDI-MS technique.[13,18b,19a] Figure S-2 (Supporting Information) reveals that the HgTe nanostructures (4×) that we prepared in 300 mM ammonium citrate at pH 5.0 provided the highest signals for BSA. The interactions of BSA (pI 4.5) and HgTe nanostructures (zeta potential, −37.6 mV) were weaker, resulting in more efficient desorption. Upon increasing pH values higher than 5.0, salt induced suppression of ionization of BSA increased to a greater extent and the signal for [M + H]$^+$ ions reduced as a result of reduced proton transfer. The ionization efficiency was lower at low concentrations of HgTe nanostructures, whereas the number of BSA molecules per HgTe nanostructure was lower at high concentrations of HgTe nanostructures. We obtained only slightly different signals for the [M + H]$^+$ ion of BSA over the pH range from 4.0 to 9.0. Therefore, unlike the situation when Au NPs as matrixes are used, the pH did not play a critical role in determining the sensitivity when HgTe nanostructures are used, thereby potentially allowing detection of most biomolecules under favorable conditions.

Mass Limit and Sensitivity. Under the optimal conditions (4× HgTe nanostructures in 300 mM ammonium citrate at pH 5.0), the SALDI-MS approach allowed us to detect IgG (Figure 2). The signals at *m/z* 149 993, 75 012, 49 990, and 37 502 represent the [M + H]$^+$, [M + 2H]$^{2+}$, [M + 3H]$^{3+}$, and [M + 4H]$^{4+}$ adducts of IgG, respectively. The broad peak (marked as *) at *m/z* around 25 000 Da is attributed to the quasimolecular ions of two identical light chains of IgG. To the best of our knowledge, this finding is the first example of the use of nanomaterials as SALDI-MS matrixes for the detection of analytes having a value of *m/z* close to 150 000 Da.[6−20]

To further demonstrate the features of the HgTe matrixes, we tested the sensitivity of SALDI-MS toward a number of standard peptides and proteins. Figure 3 reveals peaks for the [M + H]$^+$ ions, rather than the corresponding alkali-adducted analyte ions, in the SALDI mass spectra of angiotensin I, insulin, cytochrome C, and hCAI. In addition, a peak for the [M + 2H]$^{2+}$ ion appeared only for hCAI.

Table 1 lists the concentration LODs and linear ranges of these four analytes and BSA obtained through SALDI-MS when HgTe nanostructures are used. The LOD in term of absolute amount for angiotensin I was about 10 fmol, which is comparable to that using α-cyano-4-hydroxycinnamic acid as matrixes. To further improve the concentration sensitivity, we applied the HgTe nanostructures as concentrating probes, and Table 1 reveals that the concentration LODs decreased by a factor of at most 50 times after conducting the concentration process. The concentration LOD was down to 200 pM for angiotensin I. The relative standard deviations (RSDs) of the signal intensities of BSA collected from 20 different sample spots using the HgTe nanostructures and SA as matrixes were 24 and 67%, respectively. The better reproducibility of the former was mainly the result of improved sample homogeneity. In addition, preparing the analytical samples using the HgTe nanostructures as the matrix is a much simpler process.

Table 1. Linear Ranges (LRs) and LODs of Peptides and Proteins Using SALDI-MS and MALDI-MS

	HgTe[a]			HgTe[b]			organic matrixes	
analyte	LR (μM)	R^2	LOD (nM)[c]	LR (μM)	R^2	LOD (nM)[c]	LOD (nM)[c]	concentration factor[d]
angiotensin I	0.05–2.5	0.9961	10	0.001–0.1	0.9989	0.2	12[e]	50.0
insulin	0.5–25	0.9866	125	0.01–0.5	0.9882	3.3	128[f]	37.9
cytochrome C	0.2–25	0.9987	50	0.005–0.5	0.9898	1.6	125[f]	31.3
hCAI	0.5–50	0.9989	140	0.02–1.0	0.9931	4.5	210[f]	31.1
BSA	2–75	0.9897	452	0.1–5.0	0.9929	14	420[f]	32.3

[a] Analytical procedure is described in the Experimental Section. [b] Concentration of the analytes was measured prior to SALDI-MS analysis. [c] Concentration limit of detection. [d] The ratio of the concentration LOD of the analyte obtained without the use of HgTe as concentration probes over that obtained with the use of HgTe as concentration probes. [e] CHCA (10 mg/mL in water/ACN (1:1, v/v) containing 0.1% TFA) was used as the matrix. [f] SA (20 mg/mL in water/ACN (1:1, v/v) containing 0.1% TFA) was used as the matrix.

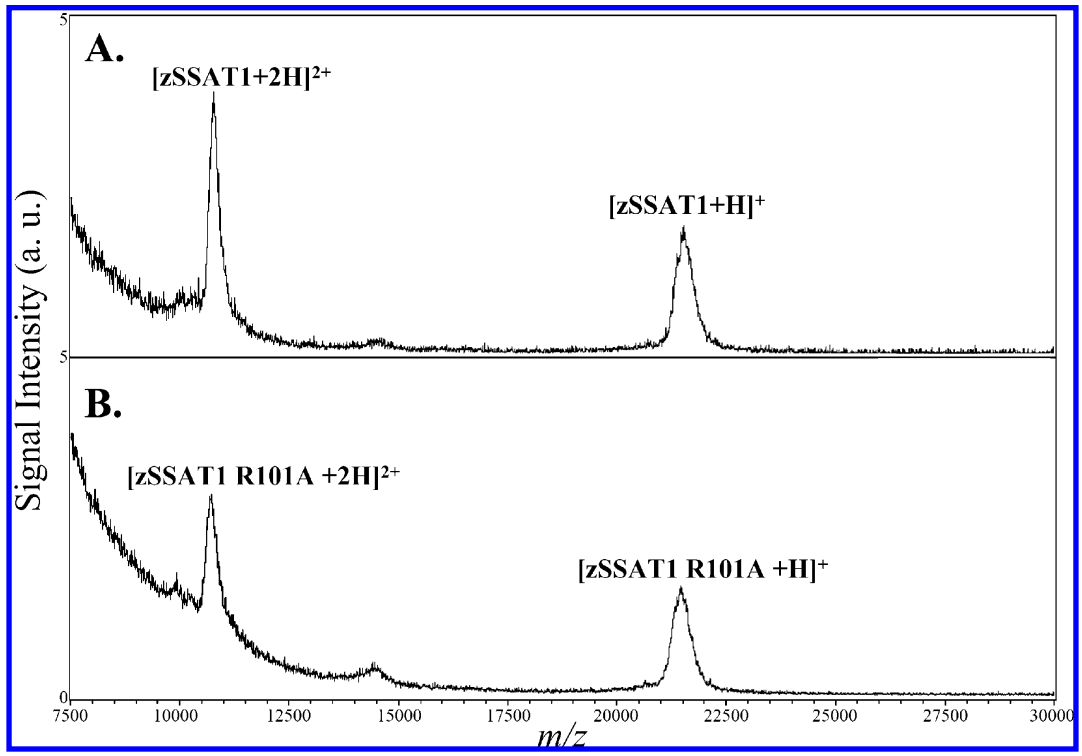

Figure 4. Mass spectra of solutions containing HgTe nanostructures and the recombination proteins (0.01 μg/μL) (A) zSSAT1 and (B) zSSAT1 R101A. SALDI-MS was performed in the linear mode. The peaks at *m/z* 10 770, 21 539, 10 728, and 21 454 represent the adducts $[zSSAT1 + 2H]^{2+}$, $[zSSAT1 + H]^{+}$, $[zSSAT1\ R101A + 2H]^{2+}$, and $[zSSAT1\ R101A + H]^{+}$, respectively. Other conditions were the same as those described in Figure 1.

Practicality. To test the practicality of the use of the HgTe nanostructures as matrixes for the detection of proteins in biological systems, we detected proteins expressed in *E. coli*. Figure 4 reveals the presence of peaks at *m/z* 10 770, 21 539, 10 728, and 21 454 that correspond to the adducts $[zSSAT1 + 2H]^{2+}$, $[zSSAT1 + H]^{2+}$, $[zSSAT1\ R101A + 2H]^{2+}$, and $[zSSAT1\ R101A + H]^{+}$, respectively, resulting from the recombinant proteins of zSSAT1 or zSSAT1 R101A under individual plasmids transformed into *E. coli* strain BL21. Although zSSAT1 and zSSAT1 R101A share 99.5% amino acid sequence homology and only one amino acid variation, our approach allowed differentiation of them, showing its potential for the rapid detection of proteins.

To further test its practicality, we employed this SALDI-MS technique for the detection of protein−drug complexes. Figure 5A reveals a signal for the BSA/L-Y complex at *m/z* 66 635, corresponding to the $[M + Y + H]^{+}$ ion. Figure 5B indicates that no such signal was visible for the corresponding $[M + Y + H]^{+}$ ion from the BSA/D-Y complex, even though we had added 40 times the amount of L-Y. The formation constants for BSA/L-Y and BSA/D-Y complexes at 20 °C are 4.4×10^4 and 4.4×10^2 M^{-1}, respectively.[21] Thus, this approach provides the capability of detecting weak complexes. Notably, a MALDI-MS approach using SA as the matrix did not allow us to detect the BSA/L-Y complex, primarily because this complex is unstable under acidic conditions.[22] We also tested the MALDI-MS method using several less acidic organic matrixes, which

(21) Peters, T., Jr. *All About Albumin: Biochemistry, Genetics, and Medical Applications*; Academic Press: New York, 1996.
(22) Bo, T.; Pawliszyn, J. *J. Chromatogr., A* **2006**, *1105*, 25–32.

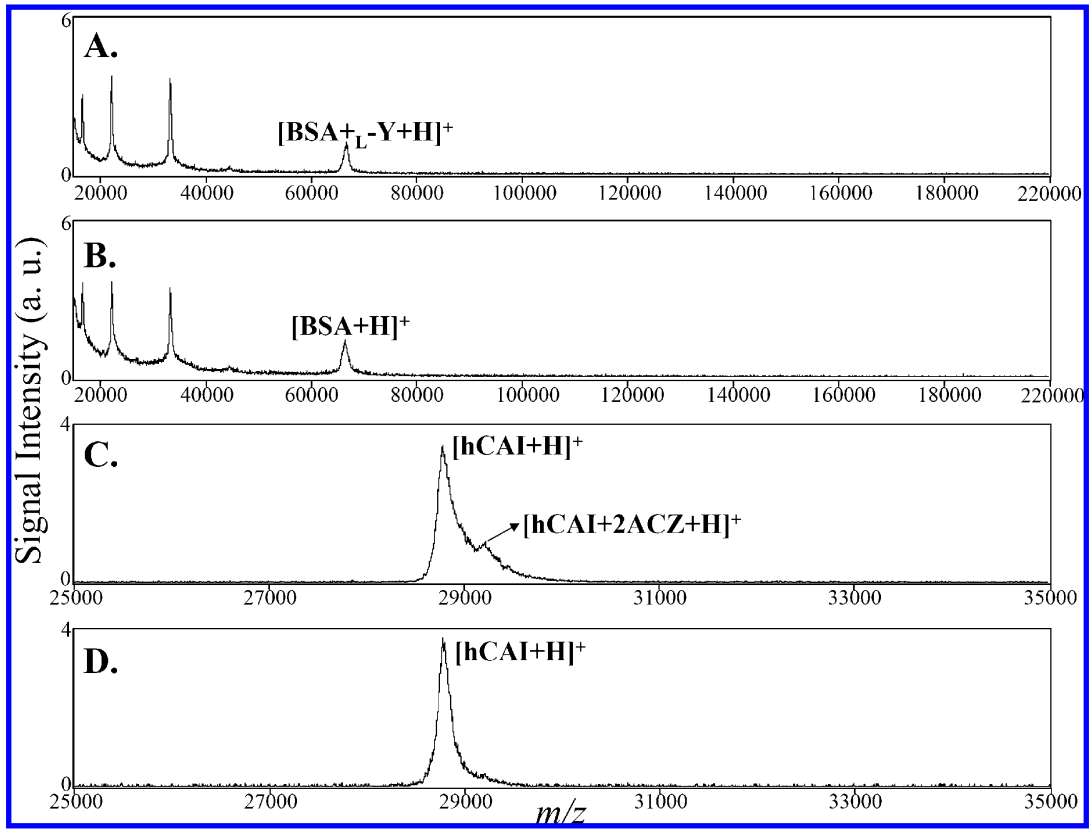

Figure 5. Mass spectra of solutions containing (A) HgTe nanostructures, BSA (5 μM), and L-Y (5 μM), prepared in 300 mM ammonium citrate buffer (pH), and (B) the mass spectrum of the same solution as that in (A), except that D-Y was added instead of L-Y. (C) Triton X-100-protected HgTe nanostructures, hCAI (5 μM), and ACZ (10 μM), prepared in 200 mM ammonium citrate buffer (pH 7.4), and (D) the mass spectrum of the same solution as that in (C), except for the absence of ACZ. SALDI-MS was performed in the linear mode. The signals at *m/z* 28 778, 29 222, 66 431, and 66 655 represent the adducts $[hCAI + H]^+$ $[hCAI + 2ACZ + H]^+$, $[BSA + H]^+$, and $[BSA + L\text{-}Y + H]^+$ respectively. Other conditions were the same as those described in Figure 1.

have been employed previously[5c,23] for the study of protein−peptide, enzyme−substrate, and enzyme−peptide complexes, for the detection of the BSA/L-Y complex, including THAP and HPA. Figure S-3 (Supporting Information) reveals that the signal at *m/z* 66 431 for the BSA/L-Y complex ($[M + H]^+$) was absent, even in the presence of 50 μM L-Y. Although the use of THAP as the matrix did not allow the detection of the BSA/L-Y complex, the charge states of the observed ions (e.g., $[M + H]^+$, $[M + 2H]^+$, and $[M + 3H]^+$; Figure S-3B, Supporting Information) were similar to those obtained through SALDI-MS when the HgTe matrix was used.

We further demonstrated the practicality of our approach through the detection of the hCAI−ACZ complex ($[hCAI + 2ACZ + H]^+$) as a signal at *m/z* 29 222 (Figure 5C). For comparison, Figure 5D displays the mass spectrum of hCAI, with a peak at *m/z* 28 778 for the $[hCAI + H]^+$ ion. To detect this complex, it was necessary for us to use a matrix of Triton X-100-protected HgTe nanostructures that had been prepared in 200 mM ammonium citrate (pH 7.4). We believe that the presence of Triton X-100 weakened the interactions between the complexes and the HgTe nanostructures and also stabilized the complexes in the gas phase. The observation of a signal for the hCAI−ACZ complex confirms that our approach has great potential for use in monitoring weak interactions between proteins and drugs.

CONCLUSION

By employing SALDI-MS with HgTe nanostructures as matrixes for the detection of proteins and protein−drug complexes, we obtained several breakthrough results. (1) The mass limit when SALDI-MS was used with HgTe nanostructures as matrixes reaches up to 150 000 Da (IgG), much higher than those obtained using other kinds of nanomaterials. (2) This SALDI-MS approach provides fewer, weaker signals from metal clusters and less interferences from metal−analyte adducts. (3) This approach provided the concentration LOD of 200 pM for angiotensin I when HgTe nanostructures were used as concentration probes and matrixes. (4) Using this SALDI-MS approach allowed us to detect weak drug−protein complexes (BSA/Y and hCAI−ACZ complexes). Furthermore, the advantages of employing SALDI-MS with HgTe nanostructures as matrixes, rather than conventional organic matrixes, are low variation between runs (RSD: <25%), simple sample preparation, and operation under sample-friendly conditions. We anticipate that the combination of SALDI-MS with HgTe nanostructures as matrixes will open new ways for proteomics and investigations of protein−drug complexes.

(23) (a) Wang, Z.; Yu, X.; Cui, M.; Liu, Z.; Song, F.; Liu, S. *J. Am. Soc. Mass Spectrom.* **2009**, *20*, 576–583. (b) Friess, S. D.; Daniel, J. M.; Hartmann, R.; Zenobi, R. *Int. J. Mass Spectrom.* **2002**, *219*, 269–281. (c) Woods, A. S.; Buchsbaum, J. C.; Worrall, T. A.; Berg, J. M.; Cotter, R. J. *Anal. Chem.* **1995**, *67*, 4462–4465.

ACKNOWLEDGMENT

This study was supported by the National Science Council of Taiwan under contract NSC 98-2113-M-002-011-MY3. Y.-W.L thanks National Taiwan University for PDF support (96R0044).

SUPPORTING INFORMATION AVAILABLE

Mass spectrum of HgTe nanomaterials prepared in 300 mM ammonium citrate (pH 5.0) (Figure S-1). Relative signal intensity of the $[M + H]^+$ ions plotted against the concentration (0−500 mM) of ammonium citrate buffer (pH 5.0) and the pH of the 300 mM ammonium citrate buffer (4.0−9.0) (Figure S-2). Mass spectra of a solution containing BSA and L-Y using organic matrixes through MALDI-MS measurements (Figure S-3). This material is available free of charge via the Internet at http://pubs.acs.org.

Received for review March 1, 2010. Accepted April 20, 2010.

AC100550C